Antarctic Science 29(4), 369–381 (2017) © Antarctic Science Ltd 2017 doi:10.1017/S0954102016000729

Tide gauge observations in Antarctica (1958–2014) and recent ice loss

G. GALASSI[1] and G. SPADA[1,2]

[1]*Dipartimento di Scienze Pure e Applicate (DiSPeA), Universita degli Studi di Urbino 'Carlo Bo', Urbino, Italy*
[2]*Istituto Nazionale di Geofisica e Vulcanologia (INGV), Bologna, Italy*
gaia.galassi@gmail.com

Abstract: Several historical sea level time series from Antarctic tide gauges, available from the Permanent Service for Mean Sea Level, are analysed. Two sea level curves, obtained by averaging data from the Antarctic Peninsula and West Antarctica, for 1958–2014, show trends of (2.0 ± 0.1) and (1.8 ± 0.2) mm yr^{-1}, respectively. By empirical mode decomposition, cyclic and non-cyclic components of sea level change were separated. A periodicity of 4–5 years was confirmed and attributed to the effects of the Antarctic Circumpolar Wave. The non-cyclic components were found to show a 'levelling off' of ≈ 1 mm yr^{-1} since *c.* 2000, which cannot be attributed to the isostatic response to Holocene ice melting. Using assessed mass balance data from the West Antarctic Ice Sheet and the Antarctic Peninsula, we studied the response to current ice loss in the region and found that the levelling off could be partly explained by accelerated melting during the last approximately two decades. This may represent the first evidence of sea level fingerprints of glacial melting in Antarctica.

Received 23 December 2015, accepted 29 November 2016, first published online 6 February 2017

Key words: Antarctic ice sheet, sea level change, tide gauge data

Introduction

Among the causes of sea level change, land-ice melting is gaining an increasing importance (see Church *et al.* 2013 and references therein). Ice mass accumulation and loss have opposite effects on sea level: an increase in accumulation causes a mean sea level fall, while an increase in surface ablation and outflow causes mean sea level to rise (Church *et al.* 2013). The melting of a land-based ice mass has several consequences. First, meltwater represents a spatially variable mass input for the oceans and causes a change in the global surface load, varying the ocean bathymetry with mantle material being forced under land masses (Fleming *et al.* 2012). Furthermore, it causes variations of the Earth's gravity fields associated with solid Earth deformations. In turn, deformational and gravitational effects cause sea level to fall near the melting sources and to rise at larger distances (Mitrovica *et al.* 2001). In addition, the slow isostatic disequilibrium of the Earth forced by the melting of the continental ice sheets causes rotational effects on large-scale sea level variations (Milne & Mitrovica 1998, Spada 2016).

The Antarctic ice sheet (AIS) is currently the largest ice reservoir on Earth. It is estimated that its complete melting would cause a global sea level rise of ~58 m (see table 4.1 in Vaughan *et al.* 2013). According to the Fifth Assessment Report (AR5) of the Intergovernmental Panel on Climate Change (IPCC), the AIS has contributed to an average sea level rise of (0.40 ± 0.20) mm yr^{-1} (probability $\geq 66\%$) during 2002–11, with a notable increase with respect to 1992–2001 $(0.27 \pm 0.11$ mm yr^{-1}, see §4.4.3 in Vaughan *et al.* 2013). Based on the previous IPCC AR4, the contribution of the AIS to sea level change was more uncertain, with (0.14 ± 0.41) mm yr^{-1} during 1961–2003 and (0.21 ± 0.35) mm yr^{-1} during 1993–2003, with a 90% confidence (see table 5.3 in Bindoff *et al.* 2007). Both reports support an acceleration in the rate of melting of the AIS and an increased confidence on its positive contribution to global sea level rise.

Despite various efforts during the last decade (see e.g. Shepherd *et al.* 2012 and reference therein), several uncertainties persist on the amount and even the sign (loss or gain) of ice mass fluxes from different sectors of the AIS. On one hand, for a warming not exceeding ~5 °C, the East Antarctic Ice Sheet (EAIS) is expected to grow by an increase in the accumulation rate (Huybrechts & de Wolde 1999). Nevertheless, according to the recent work of Golledge *et al.* (2015) a warming exceeding 1.5–2 °C above present would be sufficient to produce the collapse of large Antarctic ice shelves, with a consequent long-term 'unstoppable' contribution to sea level rise. On the other hand, in the West Antarctic Ice Sheet (WAIS) a probably irreversible mass loss is predicted for the next centuries, as a result of the relatively modest snowfall and the slow ice motion in the interior (see e.g. Golledge *et al.* 2015). An acceleration in mass loss from the AIS over the *c.* 2002–present period has been confirmed by the Gravity Recovery and Climate Experiment (GRACE) mission (see e.g. Velicogna 2009). Recently, much attention has been devoted to the Antarctic Peninsula (AP), where there is

https://doi.org/10.1017/S0954102016000729 Published online by Cambridge University Press

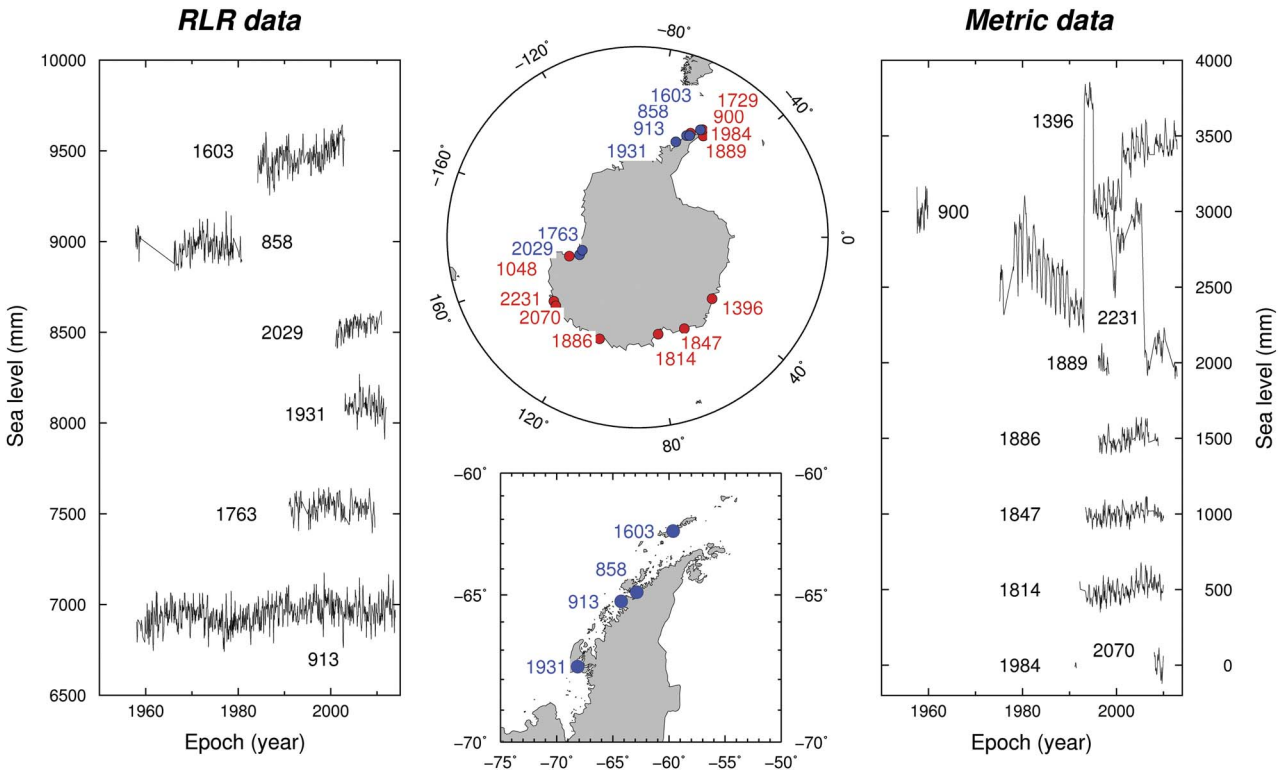

Fig. 1. Location of the Permanent Service for Mean Sea Level (PSMSL) tide gauge (TG) stations available for Antarctica (middle). Red and blue dots show the Metric and Revised Local Reference (RLR) stations, respectively, with the corresponding time series shown in the left and right frames. These have been shifted by 500 mm along the y-axis for the purpose of visualization. The Metric records for id. 1048 and 1729 (namely, McMurdo Sound and Artigas) are not shown because they are highly anomalous.

strong evidence that regional warming and increased meltwater ponding has led to the collapse of several ice shelves and the consequent acceleration of their associated outlet glaciers (see e.g. Scambos *et al.* 2003).

It has been suggested that, in principle, sea level signals recorded by tide gauges (TGs) can be used to assess recent changes in the mass balance of ice sheets or glaciers (Mitrovica *et al.* 2001, Douglas 2008). On a short timescale (years to decades) the Earth responds elastically to the removal of surface loads, which causes a variation of relative sea level at the coasts. Hence it is expected that observations from TGs located in the vicinity of major ice sheets could be useful to constrain the recent time-history of their mass unbalance (Bindoff *et al.* 2007). However, the effective observation of changes in the mass balance of ice sheets by means of TGs is limited by various problems. In particular, at the end of the 1990s the state of polar TGs was generally unsatisfactory. The subject was first reviewed by Plag (2000), who pointed out the degradation of the observation system and emphasized the importance of Arctic data for the understanding of the ongoing climate variations. The problem of the Arctic sea level observations has been recently reassessed by Henry *et al.* (2012).

Despite the importance of instrumental measurements in the vicinity of the ice margins, the interest in Antarctic TGs has apparently declined over the years. The most recent review on the topic, which dates back to the work of Lutjeharms *et al.* (1985), has evidenced a poor coverage of continuous observations. Recent work on geodetic and tidal measurements in Antarctica (Capra & Dietrich 2008) has not addressed the general state of the long-term instrumental observations in the region. Some authors (e.g. King & Padman 2005) have focused attention on short time series (a few weeks to months) in order to calibrate ocean tide models, but these are not useful to study long-term sea level trends. In recent years, the Scientific Committee on Antarctic Research has activated projects involving TG observations but no substantial changes have occurred. Currently, most of Antarctic TGs have discontinuous records or are no longer operative (see http://www.psmsl.org and King & Padman 2005).

Here, we use the most reliable TG observations from Antarctica, held by the Permanent Service for Mean Sea Level (PSMSL). The PSMSL database contains relative sea level information for 17 stations, mostly located across the AP (8 out of 17, see Fig. 1). For six of them, Revised Local Reference (RLR) monthly and yearly observations are available, spanning from year 1957.79 (Almirante Brown) to 2013.95 (Argentine Islands). For the remaining 11 stations, only 'Metric' monthly data can be obtained for

https://doi.org/10.1017/S0954102016000729 Published online by Cambridge University Press

Table I. Basic data on the Antarctic tide gauges (TGs), extracted from the Permanent Service for Mean Sea Level (PSMSL) Metric and Revised Local Reference (RLR) databases on November 2015. The locations of the TGs are also shown. N_a is the number of annual records. Where available, information of the type of instrumentation employed is also shown, obtained from the PSMSL and Scientific Committee on Antarctic Research (http://www.scar.org/).

PSMSL id.	Station name	Location	Dataset	Period	N_a (years)	Type of TG
913	Argentine Island	AP	RLR	1958–2013	54	Stilling well
1603	Puerto Soberania	AP	RLR	1984–2002	17	Pneumatic bubbler
858	Almirante Brown	AP	RLR	1958–78	11	Float
1763	Cape Roberts Antarctica	WAIS	RLR	1990–2009	14	Pressure
2029	Scott Base	WAIS	RLR	2001–10	7	Float
1931	Rothera	AP	RLR	2003–11	6	-
1984	King Sejong	AP	Metric	1991–91	0	Pressure
1889	Bahia Esperanza 2	AP	Metric	1996–98	2	-
900	Melchior	AP	Metric	1957–59	2	Float
1729	Artigas	AP	Metric	1988–89	0	-
1396	Syowa	EAIS	Metric	1975–2012	36	Pressure
1847	Davis	EAIS	Metric	1993–2010	15	-
1814	Mawson	EAIS	Metric	1992–2009	17	-
1886	Casey	EAIS	Metric	1996–2008	9	Pressure
1048	McMurdo Sound	WAIS	Metric	1963–95	1	Float
2070	Commonwealth Bay	EAIS	Metric	2008–09	2	-
2231	Dumont D'Urville	EAIS	Metric	1997–2012	10	Float

AP = Antarctic Peninsula, EAIS = East Antarctic Ice Sheet, WAIS = West Antarctic Ice Sheet.

the time window 1957–2013. According to the PSMSL recommendations (http://www.psmsl.org/data/obtaining/rlr.php), these should not be used for time series analysis. Henceforth, we assume that reliable averages of the RLR records can be obtained to characterize the sea level trend across the AP, despite different observation methods employed at different locations or changes in the instrumentation (see Table I).

Figure 1 shows the PSMSL monthly time series for stations located in Antarctica for both the RLR and Metric datasets. The record length of the available time series do not generally exceed two decades; remarkable exceptions include the RLR station of Argentine Island, located in the AP (time span: 1958–2013, record length: 54 years, completeness: 98%), and the Metric station of Syowa in East Antarctica (1975–2012, 37 years, 92%). Basic information on the Antarctica stations is listed in Table I.

The aim of this work is threefold. First, we review the existing information relating to the Antarctic TGs during the longest possible time window (1958–2014). Second, we analyse available relative sea level observations to assess their spatial and temporal variability, by studying their cyclical components and their long-term trends. Finally, we interpret the estimated levelling off of the sea level curves in terms of accelerated ice loss.

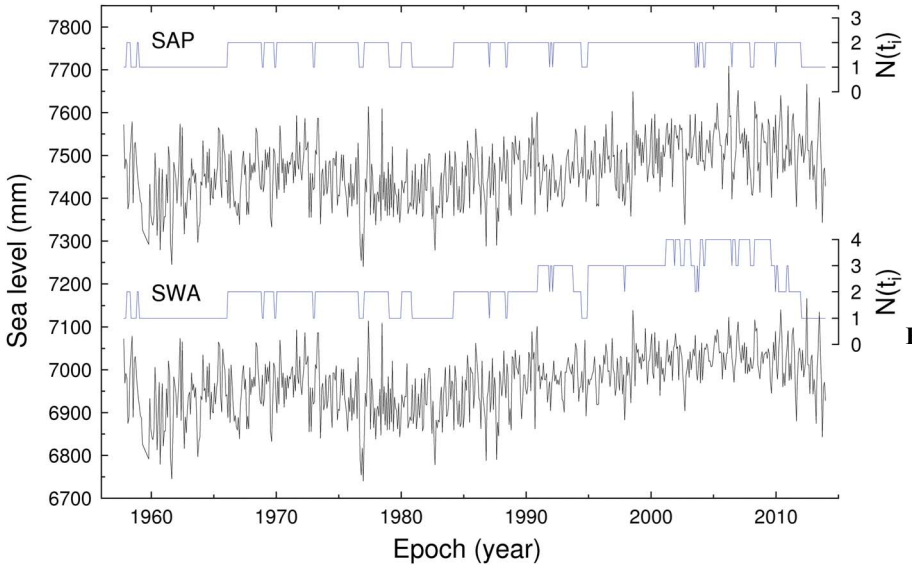

Fig. 2. Sea-level curves SWA and SAP obtained by averaging the observations from the six West Antarctic Ice Sheet Revised Local Reference (RLR) records and the four Antarctic Peninsula RLR records (see Table I), respectively. Blue lines show $N(t_i)$, which represents the number of data used, at a given epoch t_i, to compute the average in Eq. (1).

https://doi.org/10.1017/S0954102016000729 Published online by Cambridge University Press

Data and methods

Sea level time series

The limited number, short record length and the poor geographical coverage of the Antarctic TGs severely hinder a coherent visualization of the sea level variability in this region. To characterize the sea level signals available and to increase the signal-to-noise ratio, the time series are 'stacked' following the approach outlined by Olivieri & Spada (2013). In particular, for each month t_i the sea level is:

$$SL(t_i) = \frac{1}{N(t_i)} \sum_{j=1}^{N(t_i)} \left(sl_j(t_i) - \overline{sl_j} \right), \tag{1}$$

where $N(t_i)$ is the number of records for which a value of mean sea level is available, $sl_j(t_i)$ is the sea level observed at the j-th TG at time t_i and $\overline{sl_j}$ is the time-averaged sea level. Since we are considering RLR data, for which monthly (and annual) means are reduced to a common datum, in our ensuing computations the term $\overline{sl_j}$ has not been subtracted. Before evaluating Eq. (1), low-pass filters were not applied to individual time series to remove multi-decadal fluctuations because the length of the stacked curve (≈ 54 years) exceeds the absolute minimum length (50 years according to Spada & Galassi 2012) required to minimize the contamination from low-frequency decadal fluctuations.

Four out of the six RLR TGs available in the WAIS are located in the AP (see Fig. 1). This allows us to obtain from Eq. (1) two curves: SWA, drawn using the whole set of six RLR TGs and representative of the WAIS, and SAP, obtained from the four AP records. The two curves, shown in Fig. 2, share similar features to denote that records from the two WAIS stations outside the AP (namely, Cape Roberts Antarctica id. 1763 and Scott Base id. 2029) are substantially coherent with the AP observations. In the EAIS, there are no RLR stations that would allow us to obtain from Eq. (1) an average curve representative for this part of Antarctica. However, six Metric TGs time series are located in the EAIS (Fig. 1). Three of them (namely, Casey id. 1886, Davis id. 1847 and Mawson id. 1814) are fairly complete, but they are affected by several recording problems. The TG record from the site of Syowa (id. 1396) is characterized by a remarkable length (1975–2012) but shows very irregular behaviour, as can be seen in Fig. 1. More information about these stations is available from the documentation page on the PSMSL website.

The SAP and the SWA time series, as well as the individual records, have been analysed using simple regression in order to estimate their linear trend. The uncertainty (corresponding to the 95% confidence interval) is evaluated by the expressions given by Spada & Galassi (2012) i.e.:

$$\sigma_k = \frac{SEE_k}{\sqrt{\sum_j \left(t_j - \bar{t}\right)^2}}\, t_{0.975,\nu_k}, \tag{2}$$

where $\bar{t}$ is the average of t_j and $t_{0.975,\nu_k}$ is the 0.975th quartile of Student's t distribution with $\nu_k = N_k^v - 2$ df (with N_k^v being the number of valid monthly data in the k-th time series), and SEE_k is the standard error of the estimate. Since the temporal correlation of errors was not considered, the σ_k values are probably underestimated (for a complete discussion of the topic, see Bos *et al.* 2013). Here, due to the limited dataset available, trends of relatively short time span will be considered. However, we are aware that in order to avoid the contamination of decadal oscillations in the computed sea level trend, it is necessary to employ series with a minimum length of some decades (see e.g. Sturges & Hong 2001). The stacking of relatively short time series can, at least partly, alleviate this problem.

To enlighten the possible existence of cyclic components in the observed sea level signals, we apply the empirical mode decomposition (EMD) method of Huang *et al.* (1998). Here, an improved version of the method was used (the 'ensemble EMD', hereafter EEMD, see Wu & Huang 2009), and in particular the Complete Ensemble EMD with Adaptive Noise described and implemented in MATLAB by Torres *et al.* (2011). This same approach has been adopted by different authors to study multidecadal variations in sea level signals (e.g. see Galassi & Spada 2015 and references therein). The EEMD technique allows us to decompose non-linear and non-stationary time series $sl(t)$ according to:

$$sl(t) = \sum_{k=1}^{K} IMF_k(t) + R(t), \tag{3}$$

where the *IMF*s are a sequence of K empirically orthogonal 'intrinsic mode functions' describing cyclic (i.e. recurrent) variations. These are not necessarily characterized by constant amplitudes and phases, as is the case for the traditional Fourier approach to signal decomposition. Applying the EEMD, it is possible to isolate the non-cyclic residual $R(t)$ that reveals the long-term 'natural trend' of the time series. To avoid 'end effects' that may affect the determination of the EEMD residual a mirroring technique has been employed following Galassi & Spada (2015).

Glacial isostatic adjustment and glacial melting modelling

Since the TGs are anchored to the solid Earth, they are sensitive to vertical movements of different origins. In Antarctica, vertical movements associated with glacial isostatic adjustment (GIA) are of considerable importance (Bevis *et al.* 2009). With GIA, here we refer

https://doi.org/10.1017/S0954102016000729 Published online by Cambridge University Press

Table II. Relative sea level trends $\dot{S}$ for Antarctic tide gauge (TG) records and for their stacks SWA and SAP obtained by linear regression (the data periods are presented in Table I). The errors in the observed trend correspond to the standard deviation of the mean. Columns marked by glacial isostatic adjustment (GIA) show the GIA contribution to $\dot{S}$ at the locations of TGs, obtained according to the I5G, I6G and W12 models, respectively (the rates have been rounded to one decimal place). For SWA and SAP, the GIA value represents an average of the GIA values computed for the three models for the West Antarctica and the AP TGs, respectively. The observed rates corrected for GIA are given in the last three columns.

		Observed trend and error, mm yr^{-1}	GIA, mm yr^{-1}			Observed minus GIA, mm yr^{-1}		
			I5G	I6G	W12	I5G	I6G	W12
PSMSL id.	Station name							
913	Argentine Island	+1.4 ± 0.2	-2.2	-2.8	-1.8	+3.6	+4.2	+3.2
1603	Puerto Soberania	+6.4 ± 0.8	-1.6	-1.2	-0.9	+8.0	+7.6	+2.5
858	Almirante Brown	-1.0 ± 1.4	-2.4	-2.9	-1.8	+1.4	+1.9	+0.8
1763	Cape Roberts Antarctica	-0.3 ± 1.1	-0.6	-1.8	-3.0	+0.3	+1.5	+2.7
2029	Scott Base	+7.9 ± 2.4	+0.1	-1.4	-4.2	+7.8	+9.3	+12.1
1931	Rothera	-3.4 ± 2.2	-2.5	-2.0	-2.0	-0.9	-1.4	-1.4
Stacks								
SWA		+2.0 ± 0.1	-1.5	-2.0	-2.3	+3.5	+4.0	+4.3
SAP		+1.8 ± 0.2	-2.2	-2.2	-1.6	+4.0	+4.0	+3.4

only to the still ongoing millennial timescale response to the melting of the late-Pleistocene ice sheets (see e.g. Spada 2016 and reference therein), not including the recent changes in ice–ocean load. The latter, referred to as glacial melting (GM), will be considered separately. The GIA contribution to sea level change is usually evaluated

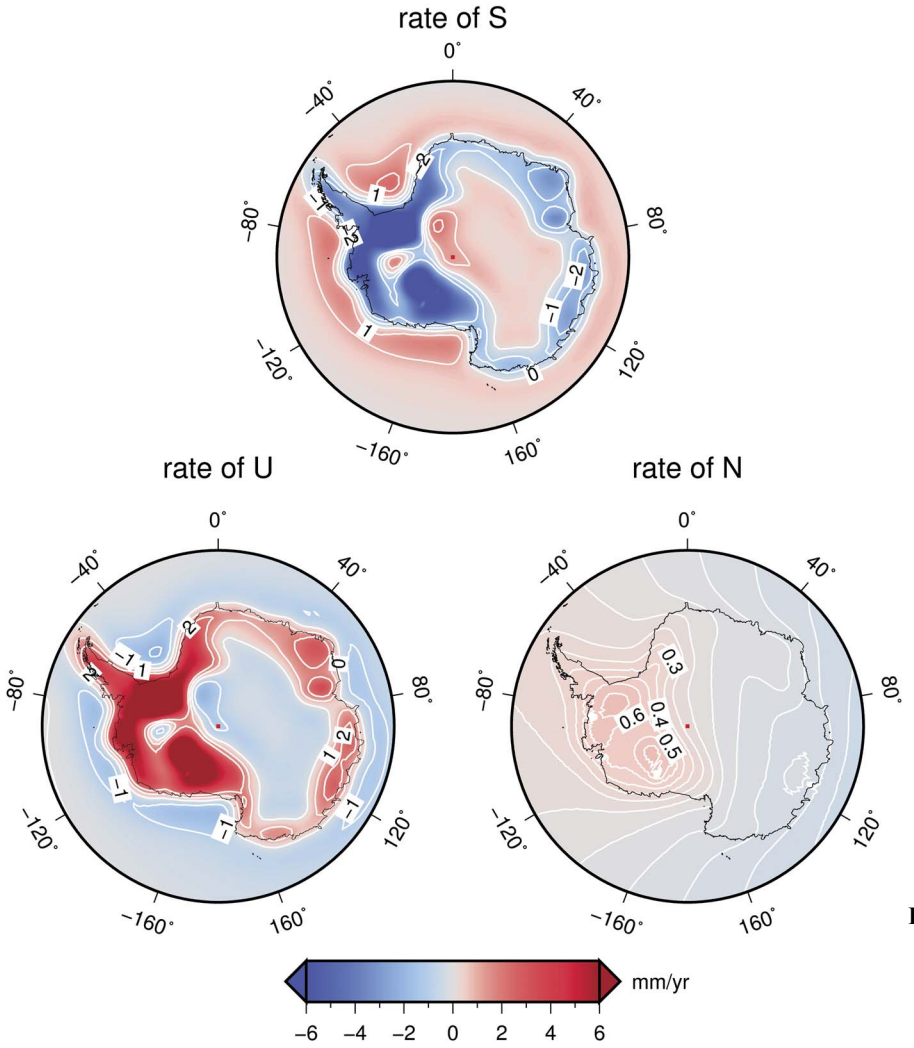

Fig. 3. Rates of relative sea level ($\dot{S}$), of vertical displacement ($\dot{U}$) and sea surface variation ($\dot{N}$) due to glacial isostatic adjustment, according to the I6G model. Units are mm yr^{-1}.

https://doi.org/10.1017/S0954102016000729 Published online by Cambridge University Press

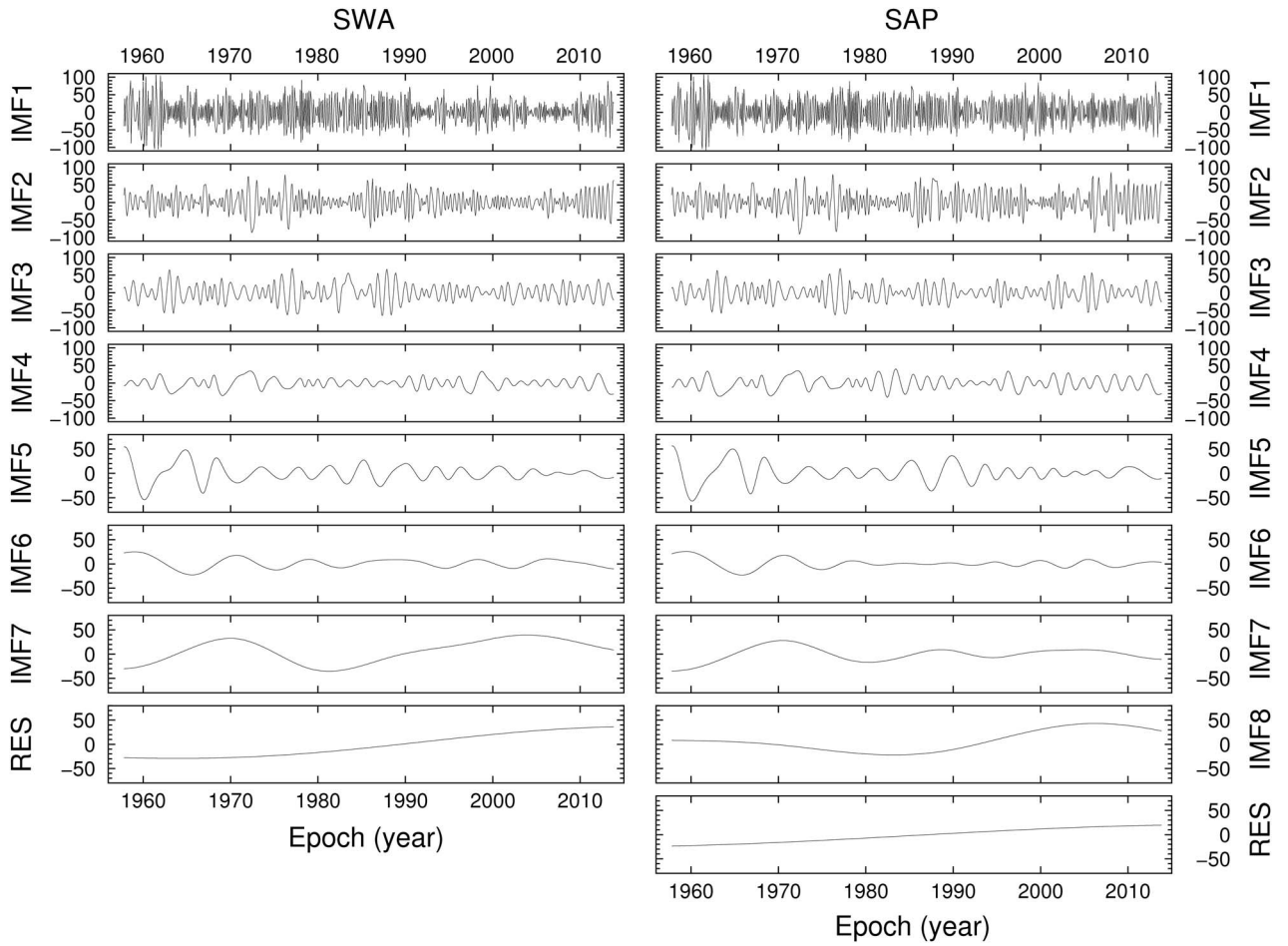

Fig. 4. Intrinsic mode functions (IMFs) and residuals (RES) obtained by ensemble empirical mode decomposition (EEMD) of the tide gauge data stacks for the West Antarctic Ice Sheet (SWA) and the Antarctic Peninsula (SAP). Units are mm.

solving the so-called 'sea level equation' (SLE) (Milne & Mitrovica 1998, Spada 2016). In terms of present-day rates of change, it reads:

$$\dot{S}(\theta,\lambda,t) = \dot{N} - \dot{U}, \tag{4}$$

where $\dot{S}$ is the rate of relative sea level change at co-latitude θ, longitude λ and at time t, $\dot{U}$ is the rate of vertical displacement of the solid surface of the Earth and $\dot{N}$ the rate of sea surface variation (i.e. absolute sea level change).

The values of $\dot{S}$ computed at the TG locations according to different global GIA models are presented in Table II. The models include ICE-5G(VM2 L90) of Peltier (2004) (hereafter, I5G), ICE-6G(VM5a) recently introduced by Peltier *et al.* (2015) (I6G) and the Antarctic deglaciation model W12 (Whitehouse *et al.* 2012). In W12, the chronology of ice sheets follows I5G outside Antarctica. According to the recent work of Purcell *et al.* (2016), the present-day radial uplift rates obtained with I6G could be overestimated along the eastern side of the AP.

To model the effects of GM, two different approaches have been followed. First, we adopted the SELEN program (Spada & Stocchi 2007), which simulates the response of the solid Earth to the melting of continental ice sheets solving the SLE. Since we are dealing with timescales of a few decades, the SLE (Eq. (4)) has been solved in the elastic approximation ignoring delayed viscoelastic effects. Furthermore, as is appropriate for large surface loads, such as the WAIS, the SLE has been solved taking the self-gravitation of the oceans into account and including the effects of Earth rotational variations (e.g. Spada 2016). Second, in order to model the effects of the localized ice loss in the AP (Nield *et al.* 2014), we used REAR (Regional ElAstic Rebound calculator), a Fortran program for computing the response of a solid, non-rotating, elastic, isotropic Earth model to surface loading (Melini *et al.* 2015). Due to the limited spatial extent of the surface load across the AP, self-gravitation of the oceans and rotational effects are not accounted for in REAR.

https://doi.org/10.1017/S0954102016000729 Published online by Cambridge University Press

Table III. Dominating period of the intrinsic mode functions (IMFs) for the sea level curves SWA and SAP. Also shown is the maximum power of the Fourier spectra of the individual IMFs.

	SWA		SAP	
IMF, n	Period, years	Max. power, $(\text{mm yr}^{-1})^2 \times 10^4$	Period, years	Max. power, $(\text{mm yr}^{-1})^2 \times 10^4$
2	0.5	1.6	0.5	2.1
3	1.0	3.2	1.0	3.0
4	1.8	2.0	3.1	0.6
5	5.0	1.8	3.9	1.5
6	11.1	0.8	9.3	1.9
7	18.5	3.6	27.8	7.6

Results

The results of the linear trend analysis on the TG series and on the SWA and SAP curves are shown in Table II. The spread of the computed trends can be attributed to different factors as the varying time ranges and record lengths, the different completeness of the time series and local processes can affect the measurements at different degrees. The rates of relative sea level change vary from negative (-3.4 mm yr^{-1} for Rothera id. 1931) to sharply positive values (+7.9 mm yr^{-1} for Scott Base id. 2029). The uncertainties are often of the order of 1 mm yr^{-1}. The longest and complete time series (Argentine Island id. 913), shows a trend of +1.4 mm yr^{-1} for the period

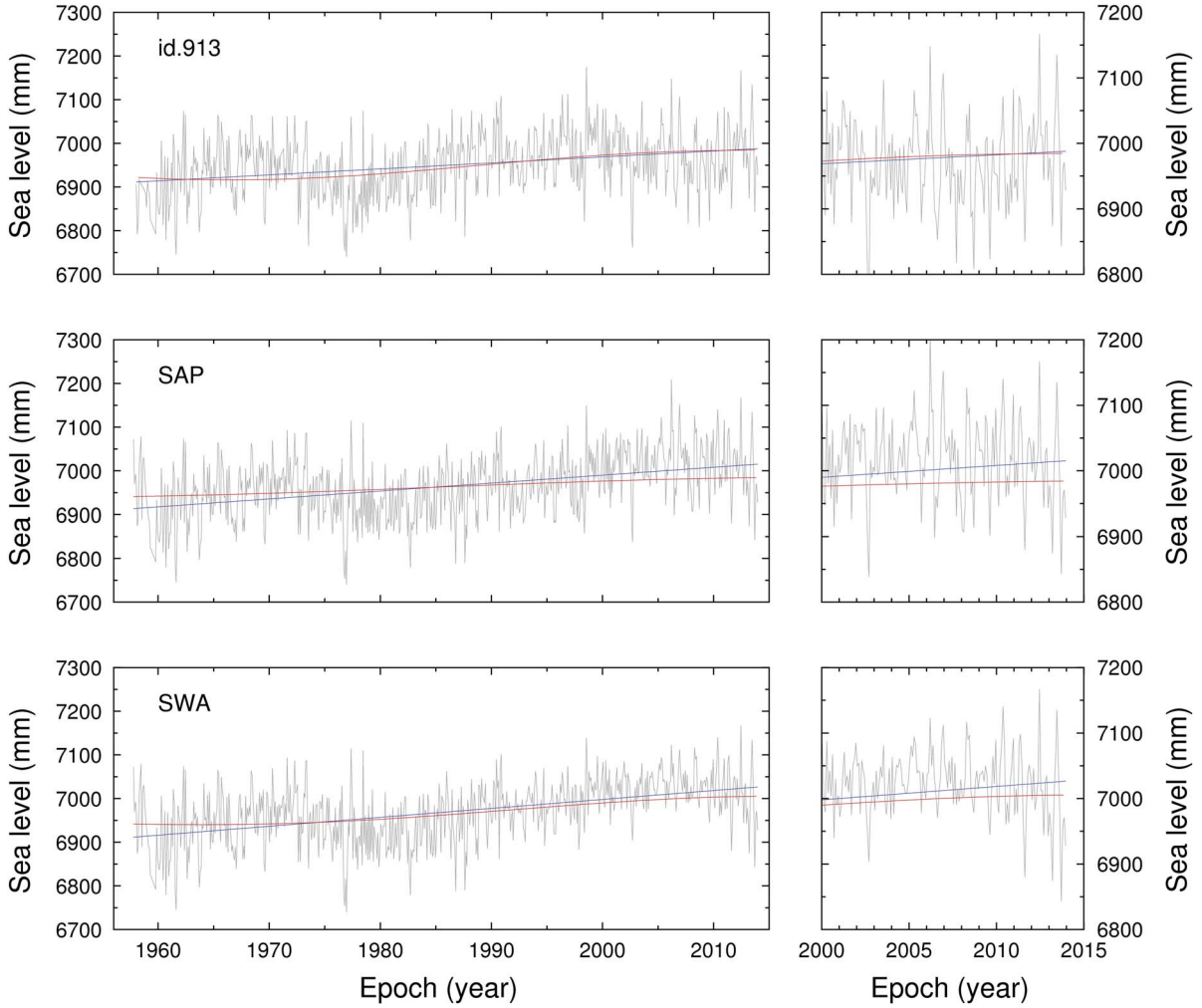

Fig. 5. Linear trend (blue) and ensemble empirical mode decomposition (EEMD) residuals (red) for the Argentine Island tide gauge (id. 913), SAP and SWA. The frames on the right show of the curves during last ~15 years.

https://doi.org/10.1017/S0954102016000729 Published online by Cambridge University Press

1958–2013; in this case the uncertainty is relatively small (0.2 mm yr^{-1}). During this time span, the linear trends are (2.0 ± 0.1) mm yr^{-1} for the SWA curve and (1.8 ± 0.2) mm yr^{-1} for the SAP.

The fields (or 'GIA fingerprints') corresponding to the I6G model are shown in Fig. 3. Note that in the bulk of the WAIS the rate of vertical uplift is $\dot{U} \approx -\dot{S}$, characteristic of regions subject to strong post-glacial rebound. Values of $\dot{S}$ associated with GIA at the locations of the TGs considered in this study (see Table II) are all negative (with the exception of the I5G value at the Scott Base TG) and are within the range of -4.2 – -0.6 mm yr^{-1}. A comparison with the observed rates in the first column confirms the significant contribution of GIA at all the Antarctic TGs. The GIA values representative of the sea level variations occurring in West Antarctica and the AP have been obtained by averaging the I6G modelled values of $\dot{S}$ at the TG locations, based on the fingerprints shown in Fig. 3. By subtracting the average I6G GIA contribution (-2.0 mm yr^{-1} for SWA and -2.2 mm yr^{-1} for SAP) from the observed sea level trends of the two curves, a value of 4.0 mm yr^{-1} is obtained for $\dot{S}$ for both.

The results of the EEMD of the SWA and the SAP time series are shown in Fig. 4 and Table III; the peak values of the power of their Fourier spectra are also shown in Table III. The first two IMFs of both curves capture the semi-annual and the annual periodicities of the sea level signals while the others reveal oscillations with longer periods. Both the SAP and the SWA show a relatively energetic component (IMF5) with a period of ~4–5 years (Table III). By further computations, the same periodicity has been detected in a stacked sea level curve composed of some RLR records from southern Patagonia (i.e. Puerto Williams, Ushuaia II, Diego Ramirez, Punta Arenas, Ushuaia I and Caleta Percy). The residuals for SWA and SAP are obtained by removing all the cyclical IMF components from the stacked time series, (shown in the bottom frames of Fig. 4).

Discussion

Concerning the long-term trends and the periodicities of the sea level signals, the above results require some discussion. The GIA-corrected (I6G) linear trends obtained for the SWA and SAP curves (4.0 mm yr^{-1}), can be interpreted as the result of GM and of thermosteric and halosteric oceanic contributions (Spada & Galassi 2012). In addition, these rates can be influenced by the feedback mechanism between temperature and salinity

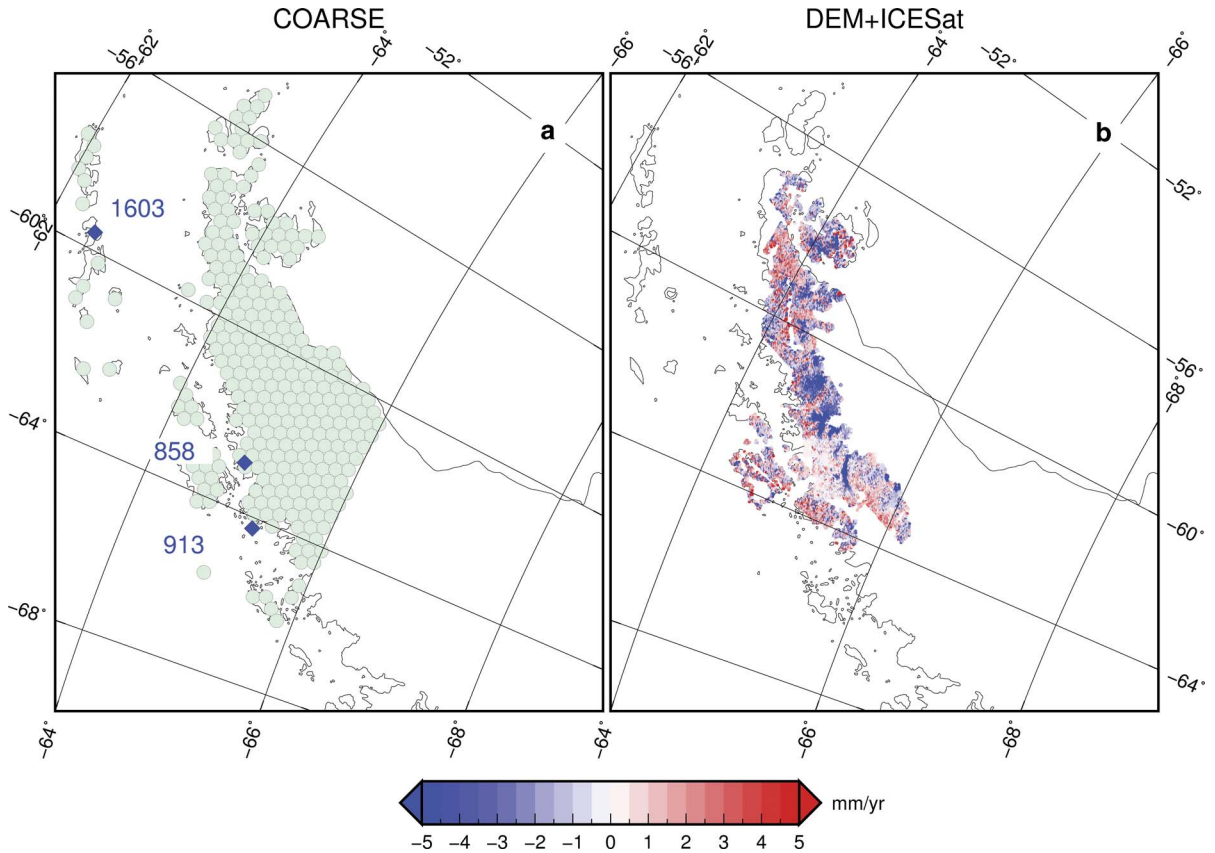

Fig. 6. Ice distribution and rate of ice loss (in Gt yr^{-1}) for **a.** 'coarse' distribution and **b.** the DEM + ICESat-based model used in Nield *et al.* (2014). The locations of the Revised Local Reference (RLR) tide gauges are also shown.

https://doi.org/10.1017/S0954102016000729 Published online by Cambridge University Press

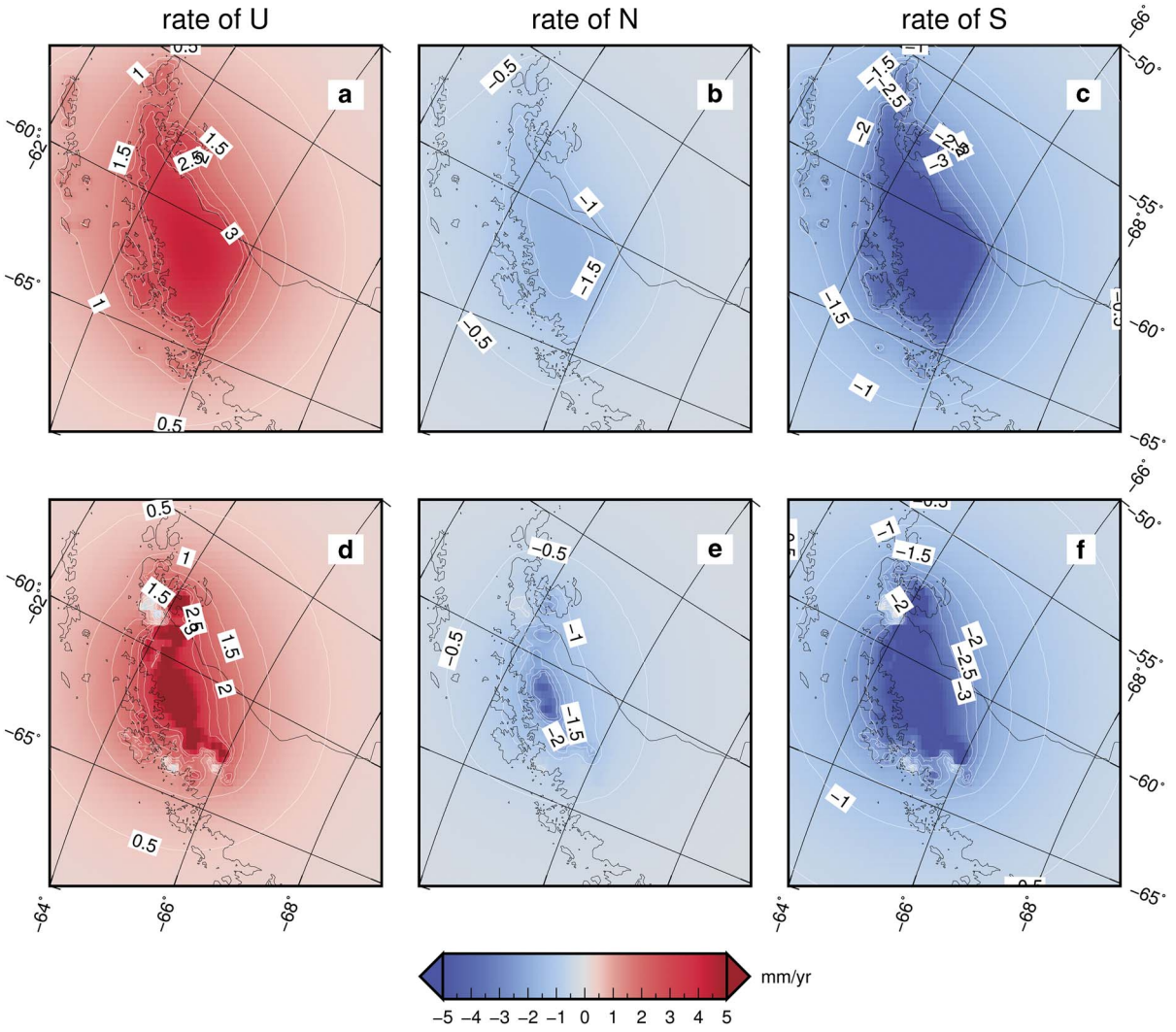

Fig. 7. Rates of vertical displacement ($\dot{U}$), sea surface variation ($\dot{N}$) and relative sea-level change ($\dot{S} = \dot{N} - \dot{U}$), modelled by the REAR program for an ice melt rate of 20 Gt yr^{-1} uniformly distributed across the Antarctic Peninsula (**a.**–**c.**) and for the Nield *et al.* (2014) ice mass balance and distribution (**d.**–**f.**).

trends and sea ice production (see, for the AP, Meredith & King 2005). The 4–5 year component of the SWA and SAP time series has also been detected in some records from southern Patagonia, with a comparable period characterizing the propagation of the Antarctic Circumpolar Wave (~4–5 years, see White & Peterson 1996). This is responsible for interannual variations in the atmospheric pressure at sea level, wind stress and sea surface temperature with a westward propagation. The connection between ice dynamics, sea level rise and the circumpolar wave in Antarctica has been recently assessed by Mémin *et al.* (2015).

In Fig. 5, the EMD residuals obtained for the SWA and for the SAP (red) are compared, with the trend obtained by a simple regression (blue), during the period (1958–2014). It is apparent that during the last few decades the EMD residual shows a reduced rate of variation (i.e. a levelling off) with respect to the long-term linear trend. Considering only 2000–14, the trend of the SAP residual is 0.6 mm yr^{-1}, i.e. 1.2 mm yr^{-1} smaller than that shown by the linear model over the whole time window (1.8 ± 0.2 mm yr^{-1}). For the SWA, the 2000–14 trend of the residual is 1.2 mm yr^{-1}, reduced by 0.9 mm yr^{-1} relative to the long-term linear trend. A similar deviation from the linear trend is also visible in the first part of the curves (1960–70), which could be explained by an accelerated ice mass loss, possibly occurring locally. Unfortunately, the limited knowledge about the melting history of Antarctica during this period makes further investigations impossible.

Since the GIA contribution to sea level change can be considered constant on the timescales of a few decades because of the relatively high viscosity values commonly employed in modelling (see e.g. Spada *et al.* 2014), the apparent levelling off observed for both curves since 2000

https://doi.org/10.1017/S0954102016000729 Published online by Cambridge University Press

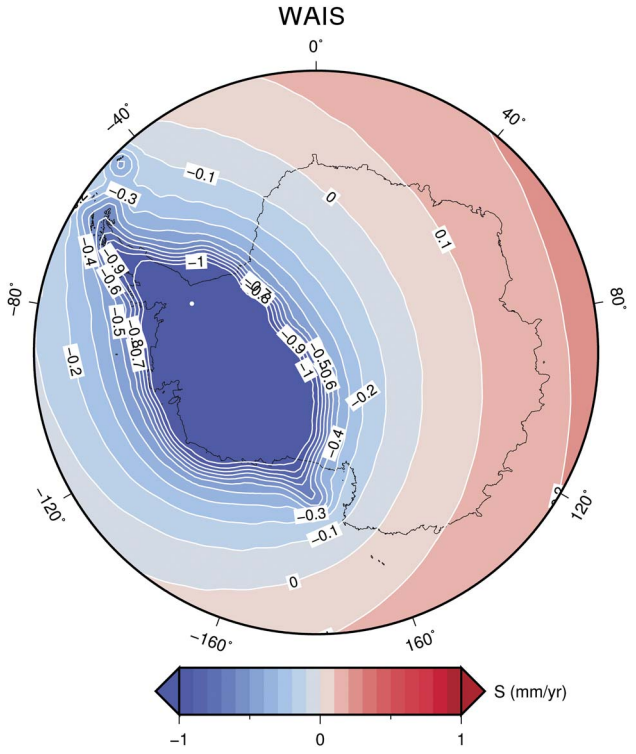

Fig. 8. Rate of relative sea-level change ($\dot{S}$, in mm yr^{-1}) due to melting of the West Antarctic Ice Sheet (WAIS), modelled by SELEN assuming a uniformly distributed rate of ice loss of 85 Gt yr^{-1}.

cannot be attributed to GIA. It is therefore possible that these anomalies in the observed trends have been caused by the recent ice melting, which can produce short-term elastic or viscoelastic deformations and, consequently, relative sea level variations. In his work, Douglas (2008) already addressed the question of the detectability of sea level fingerprints of the current melting in Antarctica. However, he employed TG records from relatively distant locations in Argentina, New Zealand and Australia, which he found to be contaminated by a significant decadal variability and that did not seem to indicate the presence of a fingerprint of ice loss (i.e. visible levelling offs). The large signals from the recent deglaciation in Antarctica make the local instrumental records potentially useful for the detection of fingerprints, provided that the cyclic variations are isolated and removed as it has been done here using an EEMD approach.

To address the role played by present ice melting in the observed anomalies of the residual trends, we have modelled the GM elastic response according to different geometries of unloading. As shown in the work of Nield *et al.* (2014), viscoelastic models having viscosities that are traditionally employed in global GIA studies (e.g. the VM2 viscosity profile) would not produce, on a decadal timescale, responses that differ significantly from the elastic solution. As discussed earlier, large uncertainties still exist for the mass balance of the AIS over recent decades. Different authors agree that the WAIS is losing mass faster than the EAIS, for which ice accumulation is not totally discounted (Church *et al.* 2013). Inside the WAIS, the AP is particularly sensitive to recent changes in climate conditions that have led to the retreat and to the eventual collapse of several major ice shelves over the past ~ 50 years (Berthier *et al.* 2012, Nield *et al.* 2014). Between 1993–2010, the AIS contribution to the global mean sea level budget has been assessed in 0.27 mm yr^{-1} (0.16–0.38 mm yr^{-1} with a probability $\geq$66%), corresponding to rate of ~ -97 Gt yr^{-1} (Vaughan *et al.* 2013). For the WAIS and the AP, the mass balance was assessed separately from the whole AIS by Shepherd *et al.* (2012). Accordingly, between 1992 and 2011, the mass of the WAIS (not including the AP) has changing at a rate of (-65 ± 26) Gt yr^{-1}, comparable to the whole AIS (-71 ± 53 Gt yr^{-1}). During this same period, Shepherd *et al.* (2012) have assessed a rate of mass change of (+14 ± 23) Gt yr^{-1} from the EAIS.

For the AP alone, two different ice distributions were considered. The first, referred to as 'coarse', is spatially uniform and assumes a rate of ice mass change of (-20 ± 14) Gt yr^{-1} between 1992 − 2011, in agreement with Shepherd *et al.* (2012). For the second, the detailed geometry

Table IV. Modelled values for the rate of relative sea level change ($\dot{S}$) due to melting of the West Antarctic Ice Sheet (WAIS) and the Antarctic Peninsula (AP), compared with the observed trends (from Table II). The values for WAIS have been obtained by SELEN computing the elastic response to an ice loss of 85 Gt yr^{-1}. For the AP, the 'coarse' uniform ice loss of 20 Gt yr^{-1} and the DEM + ICESat mass balance used in Nield *et al.* (2014) (~ -16 Gt yr^{-1}) are assumed. For the SWA and the SAP curves, the modelled values have been averaged at the location of tide gauges used in each stack.

		Observed trend, mm yr^{-1}	WAIS, mm yr^{-1}	AP, mm yr^{-1}	
				'Coarse'	DEM + ICESat
PSMSL id.	Station name				
913	Argentine Island	+1.4	-0.8	-2.9	-1.7
1603	Puerto Soberania	+6.4	-1.0	-1.4	-1.0
858	Almirante Brown	-1.0	-0.8	-4.8	-3.8
1763	Cape Roberts Antarctica	-0.3	-0.2	-0.1	0.0
2029	Scott Base	+7.9	-0.3	-0.1	0.0
1931	Rothera	-3.4	-0.9	-0.6	-0.5
Stacks					
SWA		+2.0	-0.5	-1.6	-1.2
SAP		+1.8	-0.6	-2.4	-1.7

https://doi.org/10.1017/S0954102016000729 Published online by Cambridge University Press

proposed by Nield *et al.* (2014) was adopted, based on elevation changes data from digital elevation model and ICESat observations (hereafter referred to as DEM + ICESat), with a mass balance of ~ -16 Gt yr^{-1} from 1996–2014. The two ice models for the AP are presented in Fig. 6, where the locations of the RLR TGs are also shown. Figure 7 shows the results of the REAR simulation using the 'coarse' distribution (Fig. 7a–c) and those of the DEM + ICESat-based model (Fig. 7d–f). In both cases, there is an intense relative sea level fall across the whole AP (Fig. 7c & f) with values of several millimetres per year along the coastlines. These patterns are strongly anti-correlated with the map of vertical uplifts induced by unloading (Fig. 7a & d). The rates of absolute sea level change (Fig. 7b & e) have a comparatively smaller amplitude, as expected in areas that are subject to intense deglaciation. The sea level fingerprint computed by SELEN assuming a uniform rate of melting across the WAIS is shown in Fig. 8. Since in this simulation the AP is included into the WAIS, the rate of ice mass change adopted corresponds to the total amount estimated by Shepherd *et al.* (2012) for the AP and the WAIS during 1992–2011, i.e. -85 Gt yr^{-1}. Across the region, significant gradients of sea level change can be observed, with values ranging between ~ -1.0 mm yr^{-1} near the load margins to ~ 0.2 mm yr^{-1} in the far field along the east coasts of Antarctica.

The modelled rates of relative sea level change computed at the TG locations are summarized in Table IV, according to the AP and WAIS ice sources considered in Figs 7 & 8, respectively. The rate of ice mass loss has been assumed constant for the TG data period. As expected, the spatial distribution of the ice sources and their mass balance influence the computed rates. At the Argentine Island and Almirante Brown TGs, the rates obtained using the 'coarse' AP source (-2.9 and -4.8 mm yr^{-1}, respectively) exceed those obtained considering the realistic DEM + ICESat-based model (-1.7 and -3.8 mm yr^{-1}, respectively). The importance of the choice of ice distribution is also reflected in the average values of the sea level fingerprints evaluated along the coastlines and at the TG locations. The averaged sea level rates computed at the TG locations for the two AP simulations is -2.4 mm yr^{-1} for the 'coarse' model and -1.7 mm yr^{-1} for the DEM + ICESat-based model. Interestingly, these rates mostly reflect the different amplitudes of the two mass balances employed, and less their spatial distribution. An average of -0.5 mm yr^{-1} was found for the WAIS.

The fingerprints shown in Figs 7 & 8 for the AP and the WAIS can help to obtain insight into the trends shown by the SWA and SAP sea level curves during last decades. From both our modelled AP fingerprints, the levelling off observed in Fig. 5 points to an accelerated melting in the AP and in particular to an increase in the rate of mass loss of ~ 10 Gt yr^{-1} in its mass balance during 2000–14, relative to 1958–2014. This is likely to be a conservative lower boundary, since our computations did not consider the amplifying effects that could be associated with the presence of a low viscosity layer beneath the lithosphere (Ivins *et al.* 2011). Indeed, Nield *et al.* (2014) demonstrated that by reducing the viscosity of the whole upper mantle to ~ 10^{18} Pa·s, the rates of uplift in response to unloading in the AP are approximately tripled with respect to a high viscosity (or elastic) mantle. They found that a very low viscosity was needed for the upper mantle to explain the rapid change in GPS uplift.

Although direct observations are not available for the AP during the entire period encompassed by the SAP TG-based curve, our estimate above supports an acceleration in the rate of melting in the AP, which has been effectively inferred from satellite data over decadal timescales (Shepherd *et al.* 2012). Indeed, according to table 1 in Shepherd *et al.* (2012), during 2000–11 the rate of mass change in the AP was estimated at (-29 ± 12) Gt yr^{-1}, significantly larger than during 1992–2000 (-8 ± 17 Gt yr^{-1}), with a corresponding increase in the rate of melting of ~ (21 ± 21) Gt yr^{-1} (the uncertainty is obtained by summing the errors in quadrature). Similarly, for the WAIS, a significant fraction of the observed levelling off shown by the SWA curve since 2000 (~ 0.9 mm yr^{-1}) could manifest the recently observed accelerated rate of ice melting across the WAIS.

According to Shepherd *et al.* (2012), it has seen a variation from (-46 ± 36) Gt yr^{-1} during 1992–2000 to (-114 ± 25) Gt yr^{-1} during 2000–11 (note these values include the contribution of the AP). The deviation from a constant rate observed in the earlier parts of the records (shown in Fig. 5) could be indicative of an early episode of deceleration in the rate of mass loss in the AP and in the WAIS, but this is not supported by direct observations.

Conclusions

All of the available RLR PSMSL records are from the WAIS, with most of them (four out of six) located in the AP. The stack of all of the RLR TGs (SWA) reveals a sea level rise of (2.0 ± 0.1) mm yr^{-1}, a value that essentially matches that obtained considering the SAP curve built from the AP records alone (1.8 ± 0.2 mm yr^{-1}). After correcting for the effects of GIA using the I6G model, the observed rate of relative sea level change is (4.0 ± 0.1) mm yr^{-1} for the SWA and (4.0 ±0.2) mm yr^{-1} for the SAP, where the uncertainty only reflects the error on the linear trend. Using other GIA models (I5G and W12), these rates would only change by 15% at most. Since 2000, the non-cyclic residual of the SAP and SWA curves obtained by an EEMD analysis, shows a levelling off of the linear trend of ~ 0.9 mm yr^{-1} for the SWA and 1.2 mm yr^{-1} for the SAP. This phenomenon could represent changes in the mass balance of melting sources located in the vicinity of the

https://doi.org/10.1017/S0954102016000729 Published online by Cambridge University Press

TGs. With the aid of the sea level fingerprints associated with the melting of ice sources in the WAIS and AP, we have shown that the recent acceleration in the rate of melting may be partly responsible of the slowing down observed in the rate of sea level rise across the AP since 2000. This may constitute the first evidence of sea level fingerprints of glacial melting in Antarctica.

Acknowledgements

We thank Matt King for providing mass balance data and very constructive comments, and two anonymous reviewers for useful suggestions. Marco Olivieri is thanked for fruitful discussions and advice. The GIA data for models ICE-5G(VM2 L90) and ICE-6G(VM5a) have been downloaded from the home page of Richard Peltier (http://www.atmosp.physics.utoronto.ca/~peltier/data.php). The W12 data have been kindly provided by Pippa Whitehouse. All the figures have been drawn using the Generic Mapping Tools (http://gmt.soest.hawaii.edu/). This work was funded by Programma Nazionale di Ricerche in Antartide (PNRA; CUP D32I14000230005) and by research grants from the Department of Pure and Applied Sciences (DiSPeA) of the Urbino University 'Carlo Bo' (CUPs H32I160000000005 and H32I15000160001). The SELEN and REAR programs can be downloaded from https://geodynamics.org/cig/software/selen/ and http://hpc.rm.ingv.it/rear, respectively.

Author contribution

Both authors contributed equally to data gathering, data analysis, figure drafting and discussion, and to the preparation of the manuscript.

References

Berthier, E., Scambos, T.A. & Shuman, C.A. 2012. Mass loss of Larsen B tributary glaciers (Antarctic Peninsula) unabated since 2002. *Geophysical Research Letters*, **39**, 10.1029/2012GL051755.

Bevis, M., Kendrick, E., Smalley, R., Dalziel, I., Caccamise, D., Sasgen, I., Helsen, M., Taylor, F.M., Zhou, H., Brown, A., Raleigh, D., Willis, M., Wilson, T. & Konfal, S. 2009. Geodetic measurements of vertical crustal velocity in West Antarctica and the implications for ice mass balance. *Geochemistry, Geophysics, Geosystems*, **10**, 10.1029/2009GC002642.

Bindoff, N., Willebrand, J., Artale, V., Cazenave, A., Gregory, J., Gulev, S., Hanawa, K., Le Qu'er'e, C., Levitus, S., Nojiri, Y., Shum, C. & Talley, L.D. 2007. Observations: oceanic climate change and sea level. *In* Solomon, S., Qin, D., Manning, M., Chen, Z., Marquis, M., Averyt, K., Tignor, M. & Miller, H., *eds. Climate change 2007: the physical science basis. Contribution of Working Group I to the Fifth Assessment Report of the Intergovernmental Panel on Climate Change*. Cambridge: Cambridge University Press, 385–432.

Bos, M.S., Fernandes, R.M.S., Williams, S.D.P. & Bastos, L. 2013. Fast error analysis of continuous GNSS observations with missing data. *Journal of Geodesy*, **87**, 351–360.

Capra, A. & Dietrich, R. 2008. *Geodetic and geophysical observations in Antarctica: an overview in the IPY perspective*. Berlin Heidelberg: Springer, 356 pp.

Church, J., Clark, P., Cazenave, A., Gregory, J., Jevrejeva, S., Levermann, A., Merrifield, M., Milne, G., Nerem, R., Nunn, P., Payne, A., Pfeffer, W., Stammer, D. & Unnikrishnan, A. 2013. Sea level change. *In* Stocker, T., Qin, D., Plattner, G.-K., Tignor, M., Allen, S., Boschung, J., Nauels, A., Xia, Y., Bex, V. & Midgley, P., *eds. Climate change 2013: the physical science basis. Contribution of Working Group I to the Fifth Assessment Report of the Intergovernmental Panel on Climate Change*. Cambridge: Cambridge University Press, 1138–1191.

Douglas, B.C. 2008. Concerning evidence for fingerprints of glacial melting. *Journal of Coastal Research*, **24**, 218–227.

Fleming, K.M., Tregoning, P., Kuhn, M., Purcell, A. & McQueen, H. 2012. The effect of melting land-based ice masses on sea-level around the Australian coastline. *Australian Journal of Earth Sciences*, **59**, 457–467.

Galassi, G. & Spada, G. 2015. Linear and non-linear sea-level variations in the Adriatic Sea from tide gauge records (1872–2012). *Annals of Geophysics*, **57**, 10.4401/ag-6536.

Golledge, N.R., Kowalewski, D.E., Naish, T.R., Levy, R.H., Fogwill, C.J. & Gasson, E.G.W. 2015. The multi-millennial Antarctic commitment to future sea-level rise. *Nature*, **526**, 10.1038/nature15706.

Henry, O., Prandi, P., Llovel, W., Cazenave, A., Jevrejeva, S., Stammer, D., Meyssignac, B. & Koldunov, N. 2012. Tide gauge-based sea level variations since 1950 along the Norwegian and Russian coasts of the Arctic Ocean: contribution of the steric and mass components. *Journal of Geophysical Research - Oceans*, **117**, 10.1029/2011JC007706.

Huang, N.E., Shen, Z., Long, S.R., Wu, M.L.C., Shih, H.H., Zheng, Q.N., Yen, N.C., Tung, C.C. & Liu, H.H. 1998. The empirical mode decomposition and the Hilbert spectrum for nonlinear and non-stationary time series analysis. *Proceedings of the Royal Society - Mathematical Physical and Engineering Sciences*, **A454**, 903–995.

Huybrechts, P. & de Wolde, J. 1999. The dynamic response of the Greenland and Antarctic ice sheets to multiple-century climatic warming. *Journal of Climate*, **12**, 2169–2188.

Ivins, E.R., Watkins, M.M., Yuan, D.-N., Dietrich, R., Casassa, G. & Rülke, A. 2011. On-land ice loss and glacial isostatic adjustment at the Drake Passage: 2003–2009. *Journal of Geophysical Research - Solid Earth*, **116**, 10.1029/2010JB007607.

King, M.A. & Padman, L. 2005. Accuracy assessment of ocean tide models around Antarctica. *Geophysical Research Letters*, **32**, 10.1029/2005GL023901.

Lutjeharms, J.R.E., Stavropoulos, C.C. & Koltermann, K.P. 1985. Tidal measurements along the Antarctic coastline. *In* Jacobs, S.S., *ed. Oceanology of the Antarctic continental shelf*. Washington, DC: American Geophysical Union, 273–289.

Melini, D., Gegout, P., King, M., Marzeion, B. & Spada, G. 2015. On the rebound: modeling Earth's ever-changing shape. *Eos*, **96**, 10.1029/2015EO033387.

Mémin, A., Flament, T., Alizier, B., Watson, C. & Rémy, F. 2015. Interannual variation of the Antarctic ice sheet from a combined analysis of satellite gravimetry and altimetry data. *Earth and Planetary Science Letters*, **422**, 150–156.

Meredith, M.P. & King, J.C. 2005. Rapid climate change in the ocean west of the Antarctic Peninsula during the second half of the 20th century. *Geophysical Research Letters*, **32**, 10.1029/2005GL024042.

Milne, G.A. & Mitrovica, J.X. 1998. Postglacial sea-level change on a rotating Earth. *Geophysical Journal International*, **133**, 10.1046/j.1365-246X.1998.1331455.x.

Mitrovica, J.X., Tamisiea, M.E., Davis, J.L. & Milne, G.A. 2001. Recent mass balance of polar ice sheets inferred from patterns of global sea-level change. *Nature*, **409**, 1026–1029.

https://doi.org/10.1017/S0954102016000729 Published online by Cambridge University Press

Nield, G.A., Barletta, V.R., Bordoni, A., King, M.A., Whitehouse, P.L., Clarke, P.J., Domack, E., Scambos, T.A. & Berthier, E. 2014. Rapid bedrock uplift in the Antarctic Peninsula explained by viscoelastic response to recent ice unloading. *Earth and Planetary Science Letters*, **397**, 32–41.

Olivieri, M. & Spada, G. 2013. Intermittent sea-level acceleration. *Global and Planetary Change*, **109**, 64–72.

Peltier, W.R. 2004. Global glacial isostasy and the surface of the ice-age Earth: the ICE-5G (VM2) model and GRACE. *Annual Review of Earth and Planetary Sciences*, **32**, 111–149.

Peltier, W., Argus, D. & Drummond, R. 2015. Space geodesy constrains ice age terminal deglaciation: the global ICE-6G C (VM5a) model. *Journal of Geophysical Research - Solid Earth*, **120**, 450–487.

Plag, H.P. 2000. *Arctic tide gauges: a status report*. Report IOC/INF-1147. Paris: Intergovernmental Oceanographic Commission of UNESCO.

Purcell, A., Tregoning, P. & Dehecq, A. 2016. An assessment of the ICE6G C (VM5a) glacial isostatic adjustment model. *Journal of Geophysical Research - Solid Earth*, **121**, 10.1002/2015JB012742.

Scambos, T., Hulbe, C. & Fahnestock, M. 2003. Climate-induced ice shelf disintegration in the Antarctic Peninsula. *In* Domack, E., Levente, A., Burnet A., Bindschadler, R., Convey P. & Kirby M., *eds. Antarctic Peninsula climate variability: historical and paleoenvironmental perspectives*. Washington, DC: American Geophysical Union, 79–92.

Shepherd, A., Ivins, E.R., Geruo, A. & 44 others. 2012. A reconciled estimate of ice-sheet mass balance. *Science*, **338**, 1183–1189.

Spada, G. 2016. Glacial isostatic adjustment and contemporary sea level rise: an overview. *Surveys in Geophysics*, 10.1007/s10712-016-9379-x.

Spada, G. & Galassi, G. 2012. New estimates of secular sea level rise from tide gauge data and GIA modelling. *Geophysical Journal International*, **191**, 1067–1094.

Spada, G. & Stocchi, P. 2007. SELEN: a Fortran 90 program for solving the 'sea-level equation'. *Computers & Geosciences*, **33**, 538–562.

Spada, G., Olivieri, M. & Galassi, G. 2014. Anomalous secular sea-level acceleration in the Baltic Sea caused by isostatic adjustment. *Annals of Geophysics*, **57**, 10.4401/ag-6548.

Sturges, W. & Hong, B.G. 2001. Decadal variability of sea level. *In* Douglas, B.C., Kearney, M.S. & Leatherman, S.P., *eds. Sea level rise: history and consequences*. San Diego, CA: Academic Press, 165–180.

Torres, M.E., Colominas, M.A., Schlotthauer, G. & Flandrin, P. 2011. A complete ensemble empirical mode decomposition with adaptive noise. *Proceedings of the Acoustics, Speech and Signal Processing (ICASSP), 2011 IEEE International Conference*, 4144–4147.

Vaughan, D.G., Comiso, J.C., Allison, I., Carrasco, J., Kaser, G., Kwok, R., Mote, P., Murray, T., Paul, F., Ren, J., Rignot, E., Solomina, O., Steffen, K. & Zhang, T. 2013. Observations: cryosphere. *In* Stocker, T.F., Qin, D., Plattner, G.-K., Tignor, M., Allen, S.K., Boschung, J., Nauels, A., Xia, Y., Bex, V. & Midgley, P.M., *eds. Climate change 2013: the physical science basis. Contribution of Working Group I to the Fifth Assessment Report of the Intergovernmental Panel on Climate Change*. Cambridge: Cambridge University Press, 317–382.

Velicogna, I. 2009. Increasing rates of ice mass loss from the Greenland and Antarctic ice sheets revealed by GRACE. *Geophysical Research Letters*, **36**, 10.1029/2009GL040222.

White, W.B. & Peterson, R.G. 1996. An Antarctic circumpolar wave in surface pressure, wind, temperature and sea-ice extent. *Nature*, **380**, 699–702.

Whitehouse, P.L., Bentley, M.J., Milne, G.A., King, M.A. & Thomas, I.D. 2012. A new glacial isostatic adjustment model for Antarctica: calibrated and tested using observations of relative sea-level change and present-day uplift rates. *Geophysical Journal International*, **190**, 1464–1482.

Wu, Z. & Huang, N.E. 2009. Ensemble empirical mode decomposition: a noise-assisted data analysis method. *Advances in Adaptive Data Analysis*, **1**, 10.1142/S1793536909000047.

https://doi.org/10.1017/S0954102016000729 Published online by Cambridge University Press